Probing inflation and reheating with gravitational waves

L. Sriramkumar

Centre for Strings, Gravitation and Cosmology, Department of Physics,
Indian Institute of Technology Madras, Chennai, India

Seminar

GreCo, Institut d'Astrophysique, Paris, France

June 3, 2024

Plan of the talk

1. Constraints on inflation from the CMB data
2. GWs provide a new window to the universe
3. Reheating can boost the strengths of primary GWs
4. Generation of GWs by enhanced scalar perturbations on small scales
5. NANOGrav 15-year data and the stochastic GW background
6. Non-Gaussianities generated in ultra slow roll and punctuated inflation
7. Loop corrections to the power spectrum due to action at the quartic order
8. Outlook

This talk is based on. . .

- M. Braglia, D. K. Hazra, F. Finelli, G. F. Smoot, L. Sriramkumar and A. A. Starobinsky, *Generating PBHs and small-scale GWs in two-field models of inflation*, JCAP **08**, 001 (2020) [arXiv:2005.02895 [astro-ph.CO]].
- H. V. Ragavendra, P. Saha, L. Sriramkumar and J. Silk, *Primordial black holes and secondary gravitational waves from ultra slow roll and punctuated inflation*, Phys. Rev. D **103**, 083510 (2021) [arXiv:2008.12202 [astro-ph.CO]].
- Md. R. Haque, D. Maity, T. Paul and L. Sriramkumar, *Decoding the phases of early and late time reheating through imprints on primordial gravitational waves*, Phys. Rev. D **104**, 063513 (2021) [arXiv:2105.09242 [astro-ph.CO]].
- H. V. Ragavendra and L. Sriramkumar, *Observational imprints of enhanced scalar power on small scales in ultra slow roll inflation and associated non-Gaussianities*, Galaxies **11**, 34 (2023) [arXiv:2301.08887 [astro-ph.CO]].
- S. Maity, H. V. Ragavendra, S. K. Sethi and L. Sriramkumar, *Loop contributions to the scalar power spectrum due to quartic order action in ultra slow roll inflation*, JCAP **05**, 046 (2024) [arXiv:2307.13636 [astro-ph.CO]].
- S. Maity, N. Bhaumik, Md. R. Haque, D. Maity and L. Sriramkumar, Constraining the history of reheating with the NANOGrav 15-year data, arXiv:2403.16963 [astro-ph.CO].

Plan of the talk

Bringing the modes inside the Hubble radius

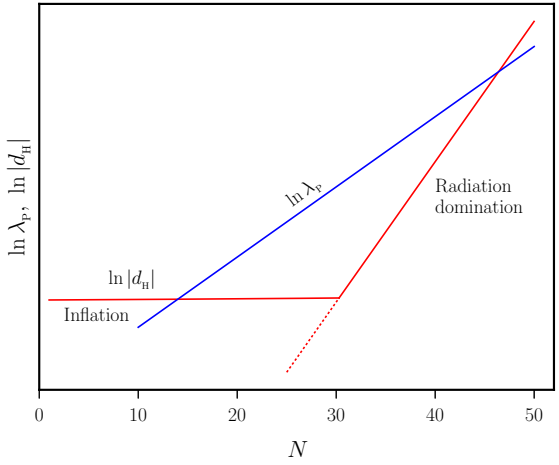

▸ Evolution of comoving lengths

The physical wavelength $\lambda_{\rm P} \propto a$ (in blue) and the Hubble radius $d_{\rm H} = H^{-1}$ (in red) in the inflationary scenario[1]. The scale factor is expressed in terms of e-folds N as $a(N) \propto {\rm e}^{N}$.

[1] See, for example, E. W. Kolb and M. S. Turner, *The Early Universe* (Addison-Wesley Publishing Company, New York, 1990), Fig. 8.4.

The inflationary attractor

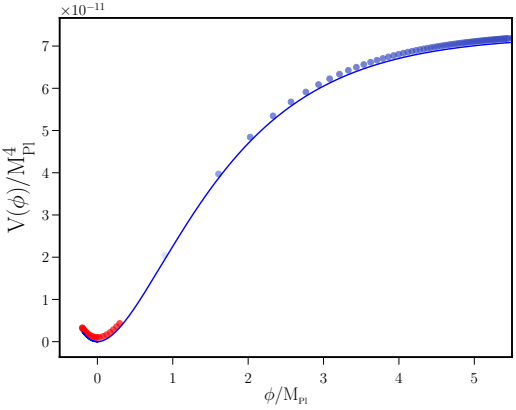

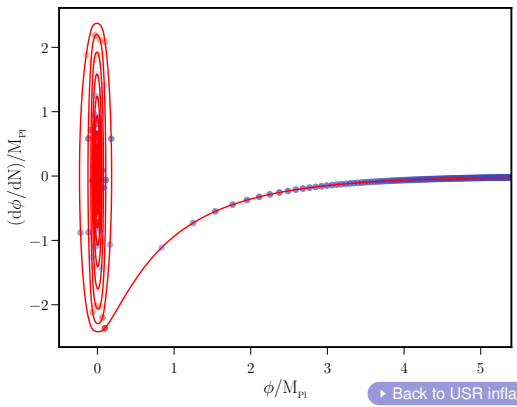

Back to USR inflation
Back to reheating

The evolution of the scalar field in the popular Starobinsky model, which leads to slow roll inflation, is indicated (as circles, in blue and red) at regular intervals of time (on the left). Illustration of the behavior of the scalar field in phase space (on the right)[2].

[2]Figure credit H. V. Ragavendra.

Performance of inflationary models in the $n_{\rm s}$-r plane

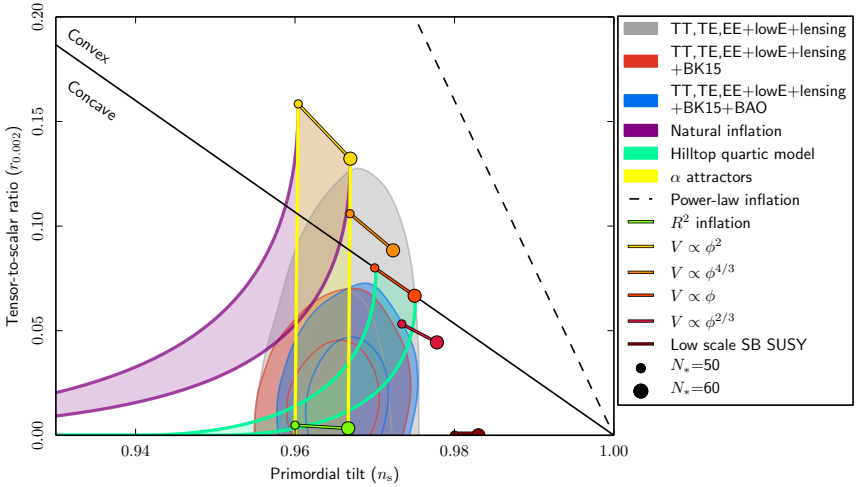

Joint constraints on $n_{\rm s}$ and $r_{0.002}$ from Planck in combination with other data sets, compared to the theoretical predictions of some of the popular inflationary models[3].

[3] Planck Collaboration (Y. Akrami *et al.*), Astron. Astrophys. **641**, A10 (2020).

Recent constraints on the tensor-to-scalar ratio r

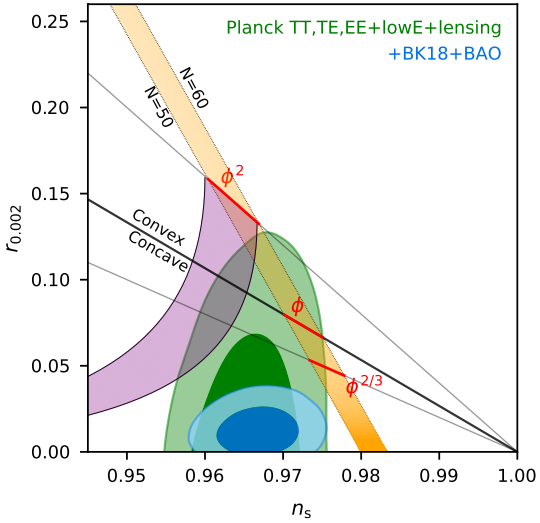

Constraints on the tensor-to-scalar ratio r from Planck and the BICEP/Keck array[4].

[4] BICEP/Keck Collaboration (P. A. R. Ade *et al.*), arXiv:2203.16556 [astro-ph.CO].

Prospects of observing the imprints of the tensor perturbations

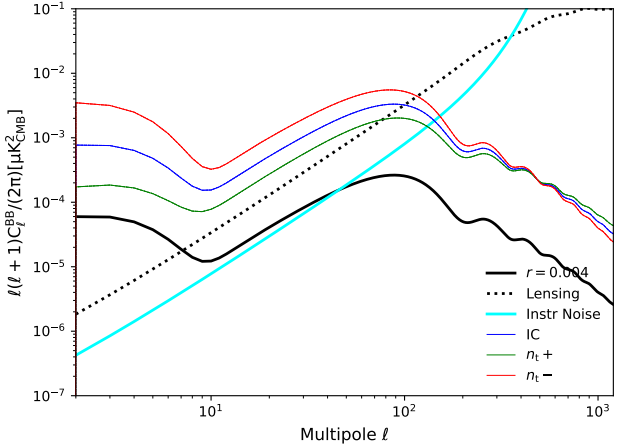

The B-mode angular power spectra of the CMB resulting from the primordial tensor perturbations for three models with $r_{0.05} = 0.05$ are plotted, along with the CMB lensing signal and the instrumental noise of a LiteBIRD-like configuration[5].

[5] D. Paoletti, F. Finelli, J. Valiviita and M. Hazumi, Phys. Rev. D **106**, 083528 (2022).

Spectra leading to an improved fit to the CMB data

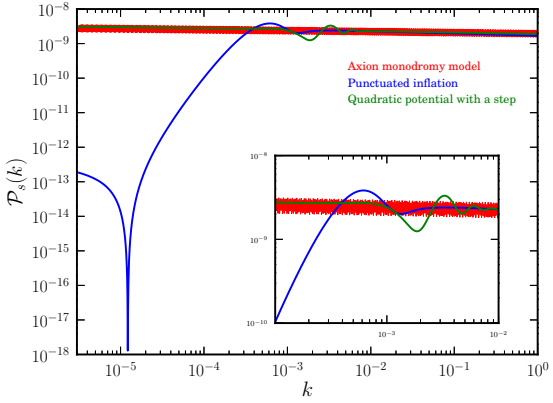

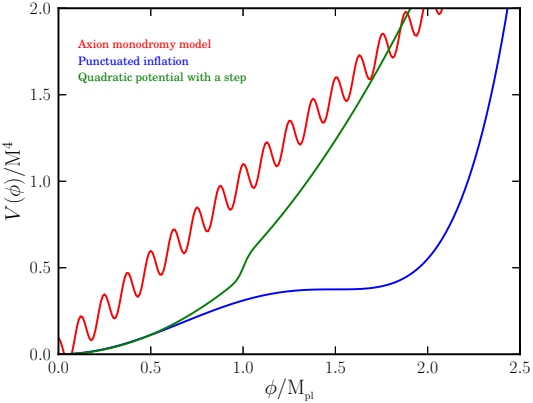

The scalar power spectra (on the left) arising in different inflationary models (on the right) that lead to a better fit to the CMB data than the conventional power law spectrum[6].

[6] R. K. Jain, P. Chingangbam, J.-O. Gong, L. Sriramkumar and T. Souradeep, JCAP **01**, 009 (2009);
D. K. Hazra, M. Aich, R. K. Jain, L. Sriramkumar and T. Souradeep, JCAP **10**, 008 (2010);
M. Aich, D. K. Hazra, L. Sriramkumar and T. Souradeep, Phys. Rev. D **87**, 083526 (2013);
For a recent discussion, see H. V. Ragavendra, D. Chowdhury and L. Sriramkumar, Phys. Rev. D **106**, 043535 (2022).

Plan of the talk

Probing the primordial universe through GWs

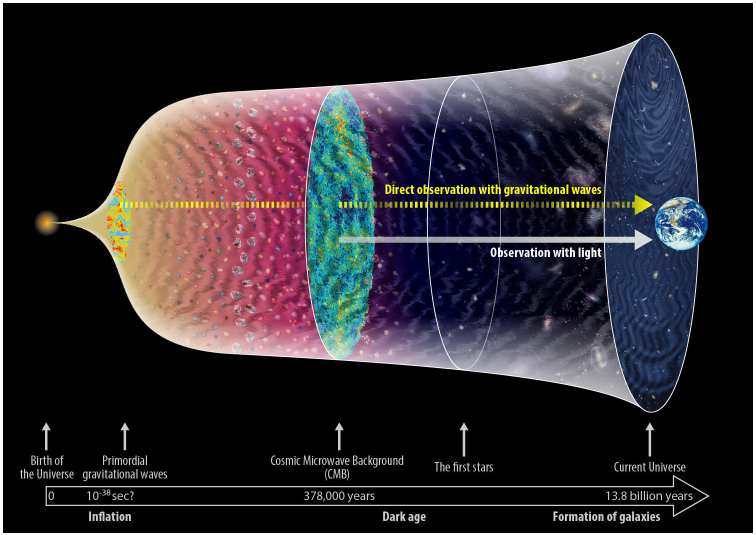

GWs provide a unique window to probe the primordial universe[7].

[7] Image from https://gwpo.nao.ac.jp/en/gallery/000061.html.

The spectrum of GWs

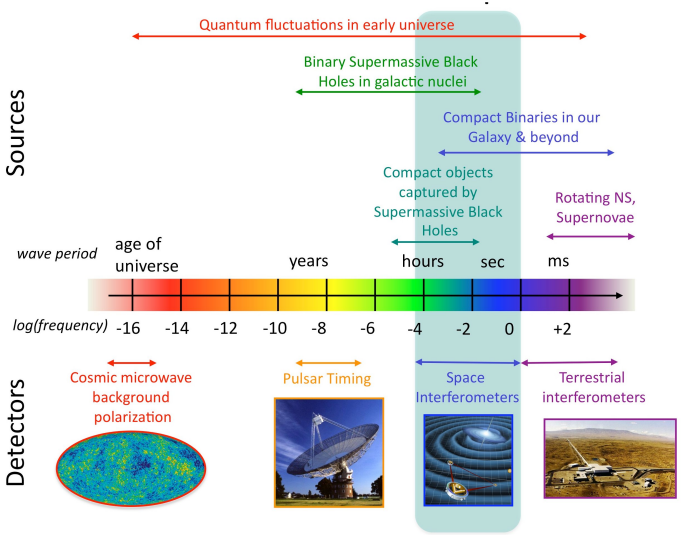

Different sources of GWs and corresponding detectors[8].

[8] J. B. Hartle, *Gravity: An Introduction to Einstein's General Relativity* (Pearson Education, Delhi, 2003).

Plan of the talk

Behavior of the comoving wave number and Hubble radius

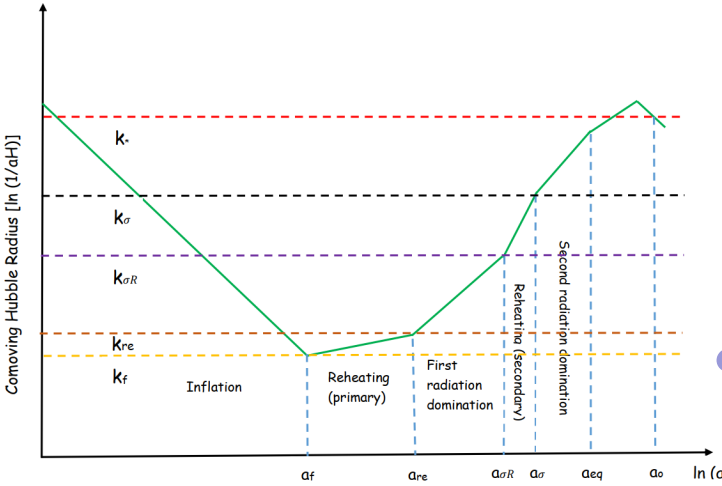

- Evolution of physical lengths
- Inflationary attractor
- Back to secondary GWs

Behavior of the comoving wave number k (horizontal lines in different colors) and the comoving Hubble radius $d_{\rm H}/a = (a\,H)^{-1}$ (in green) across different epochs[9].

[9] Md. R. Haque, D. Maity, T. Paul and L. Sriramkumar, Phys. Rev. D **104**, 063513 (2021).

Duration of reheating and the reheating temperature

The duration of the epoch of reheating $N_{\rm re}$ and the reheating temperature $T_{\rm re}$ can be expressed in terms of the equation of state parameter $w_{\rm re}$ during reheating and the inflationary parameters as follows[10]:

$$N_{\rm re} = \frac{4}{(3\,w_{\rm re}-1)}\left[N_* + \frac{1}{4}\,\ln\left(\frac{30}{\pi^2\,g_{*,\rm re}}\right) + \frac{1}{3}\ln\left(\frac{11\,g_{s,\rm re}}{43}\right) + \ln\left(\frac{k_*}{a_0\,T_0}\right) + \ln\left(\frac{\rho_{\rm e}^{1/4}}{H_{\rm I}}\right)\right],$$

$$T_{\rm re} = \left(\frac{43}{11\,g_{s,\rm re}}\right)^{1/3}\left(\frac{a_0\,H_{\rm I}}{k_*}\right)\,{\rm e}^{-(N_*+N_{\rm re})}\,T_0,$$

where $H_{\rm I}$ is the Hubble parameter during inflation, $T_0 = 2.725\,{\rm K}$ is the present temperature of the CMB, and H_0 denotes the current value of the Hubble parameter.

Note that $k_*/a_0 \simeq 0.05\,{\rm Mpc}^{-1}$ represents the CMB pivot scale and N_* denotes the number of e-folds *prior to the end of inflation* when the pivot scale leaves the Hubble radius.

[10] J. Martin and C. Ringeval, Phys. Rev. D **82**, 023511 (2010);
L. Dai, M. Kamionkowski and J. Wang, Phys. Rev. Lett. **113**, 041302 (2014);
J. L. Cook, E. Dimastrogiovanni, D. A. Easson and L. M. Krauss, JCAP **04**, 047 (2015).

Effects on $\Omega_{\rm GW}(f)$ due to reheating

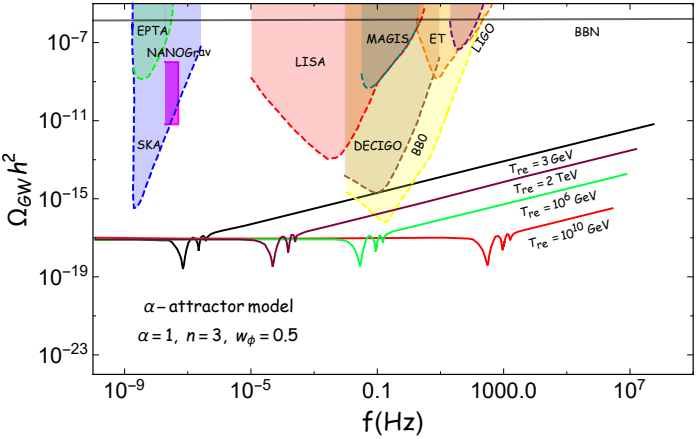

The dimensionless spectral energy density of primary GWs today, viz. $\Omega_{\rm GW}$, is plotted over a wide range of frequency f, for different reheating temperatures (in red, green, brown and black)[11]. Note that $n_{\rm GW} = 2\,(3\,w_{\rm re} - 1)/(3\,w_{\rm re} + 1)$.

[11] See, for example, K. Nakayama, S. Saito, Y. Suwa and J. Yokoyama, JCAP **0806** 020 (2008); Md. R. Haque, D. Maity, T. Paul and L. Sriramkumar, Phys. Rev. D **104**, 063513 (2021).

Effects on $\Omega_{\rm GW}(f)$ due to late time entropy production

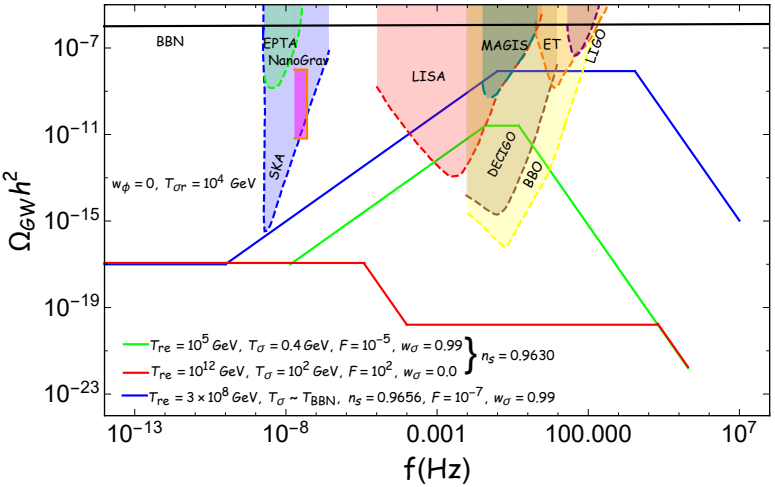

The dimensionless spectral energy density of primary GWs observed today $\Omega_{\rm GW}(f)$ is plotted in scenarios involving late time production of entropy[12].

[12] Md. R. Haque, D. Maity, T. Paul and L. Sriramkumar, Phys. Rev. D **104**, 063513 (2021).

Plan of the talk

Production of primordial black holes (PBHs) during radiation domination

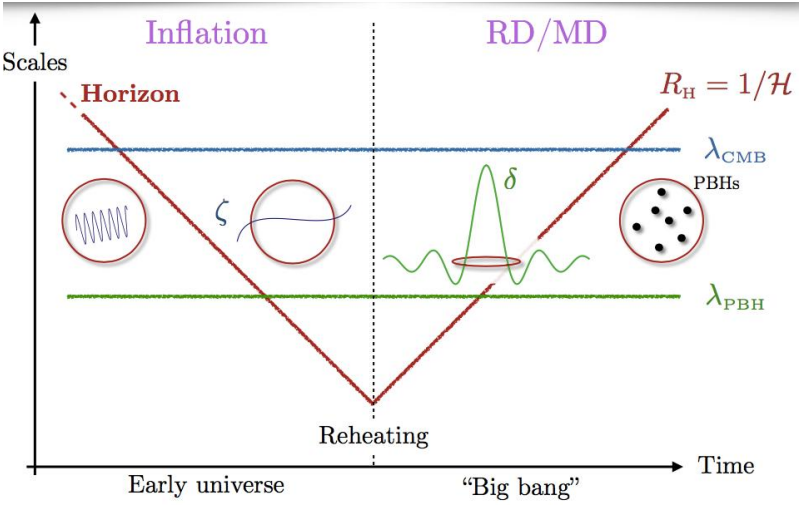

BHs can form in the primordial universe when perturbations with significant amplitudes on small scales reenter the Hubble radius during the radiation dominated epoch[13].

[13] Figure from G. Franciolini, arXiv:2110.06815 [astro-ph.CO].

Amplitude required to form significant number of PBHs

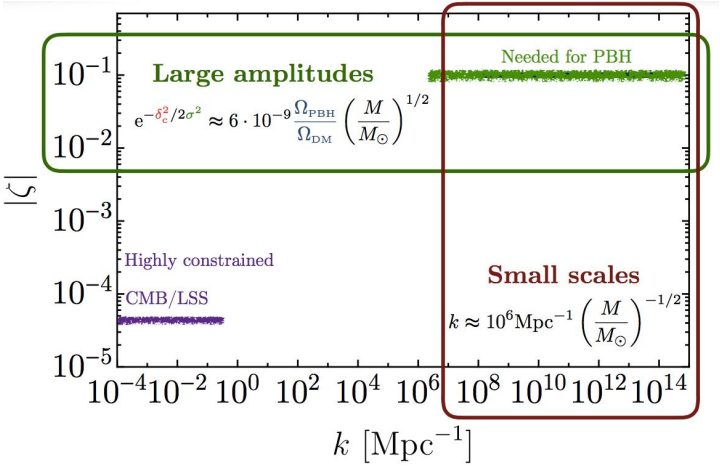

In order to form significant number of black holes, the amplitude of the perturbations on small scales has to be large enough such that the dimensionless amplitude of the scalar perturbation is close to unity[14].

[14] Figure credit G. Franciolini.

Single-field models admitting ultra slow roll inflation

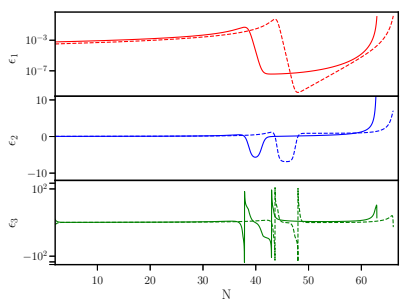

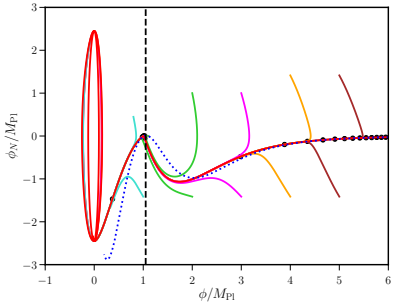

Potentials containing a point of inflection and leading to ultra slow roll inflation[15]:

▸ Inflationary attractor

$$\text{USR1}: V(\phi) = V_0\,\frac{6\,x^2 - 4\,\alpha\,x^3 + 3\,x^4}{(1+\beta\,x^2)^2}, \text{ with } x = \phi/v,\ v \text{ being a constant},$$

$$\text{USR2}: V(\phi) = V_0\left\{\tanh\left(\frac{\phi}{\sqrt{6}\,M_{\rm Pl}}\right) + A\,\sin\left[\frac{\tanh\left[\phi/\left(\sqrt{6}\,M_{\rm Pl}\right)\right]}{f_\phi}\right]\right\}^2.$$

[15] See, for example, J. Garcia-Bellido and E. R. Morales, Phys. Dark Univ. **18**, 47 (2017); C. Germani and T. Prokopec, Phys. Dark Univ. **18**, 6 (2017); I. Dalianis, A. Kehagias and G. Tringas, JCAP **01**, 037 (2019).

Single-field models permitting punctuated inflation

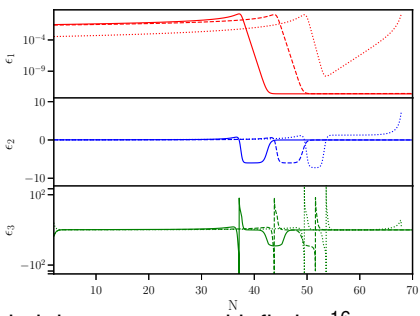

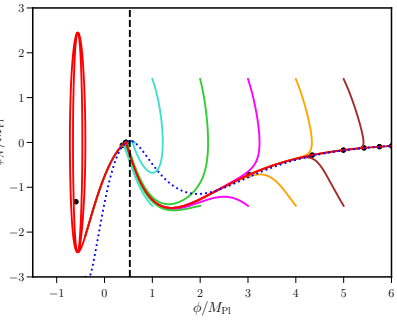

Potentials admitting punctuated inflation[16]:

$$\text{PI1}: V(\phi) \,=\, V_0\,\left(1 + B\,\phi^4\right), \quad \text{PI2}: V(\phi) = \frac{m^2}{2}\,\phi^2 - \frac{2\,m^2}{3\,\phi_0}\,\phi^3 + \frac{m^2}{4\,\phi_0^2}\,\phi^4,$$

$$\text{PI3}: V(\phi) \,=\, V_0\,\left[c_0 + c_1\,\tanh\left(\frac{\phi}{\sqrt{6\,\alpha}\,M_{_{\rm Pl}}}\right) + c_2\,\tanh^2\left(\frac{\phi}{\sqrt{6\,\alpha}\,M_{_{\rm Pl}}}\right) + c_3\,\tanh^3\left(\frac{\phi}{\sqrt{6\,\alpha}\,M_{_{\rm Pl}}}\right)\right]^2.$$

[16] D. Roberts, A. R. Liddle and D. H. Lyth, Phys. Rev. D **51**, 4122 (1995);
R. K. Jain, P. Chingangbam, J.-O. Gong, L. Sriramkumar and T. Souradeep, JCAP **01**, 009 (2009);
I. Dalianis, A. Kehagias and G. Tringas, JCAP **01**, 037 (2019).

Reconstructing scenarios of ultra slow roll and punctuated inflation

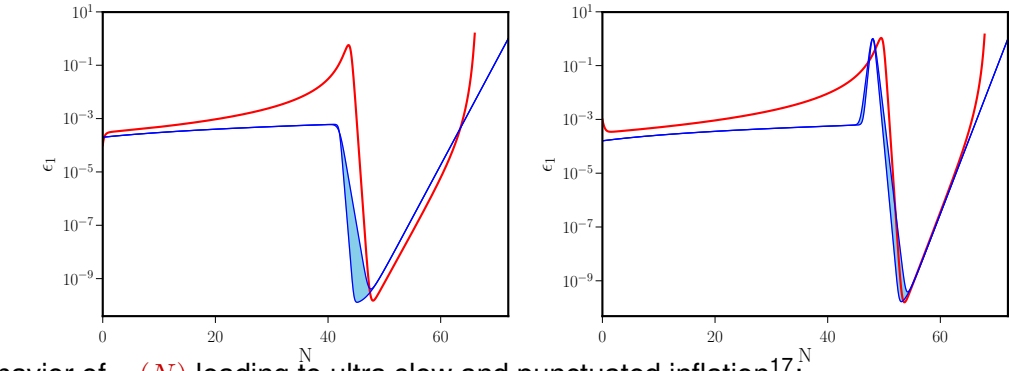

Behavior of $\epsilon_1(N)$ leading to ultra slow and punctuated inflation[17]:

$$\text{RSI}: \epsilon_1^{\text{I}}(N) = [\epsilon_{1a}\ (1+\epsilon_{2a}\,N)]\left[1-\tanh\left(\frac{N-N_1}{\Delta N_1}\right)\right]+\epsilon_{1b}+\exp\left(\frac{N-N_2}{\Delta N_2}\right),$$

$$\text{RSII}: \epsilon_1^{\text{II}}(N) = \epsilon_1^{\text{I}}(N)+\cosh^{-2}\left(\frac{N-N_1}{\Delta N_1}\right).$$

[17] H. V. Ragavendra, P. Saha, L. Sriramkumar and J. Silk, Phys. Rev. D **103**, 083510 (2021).

Power spectra in the inflationary models and reconstructed scenarios

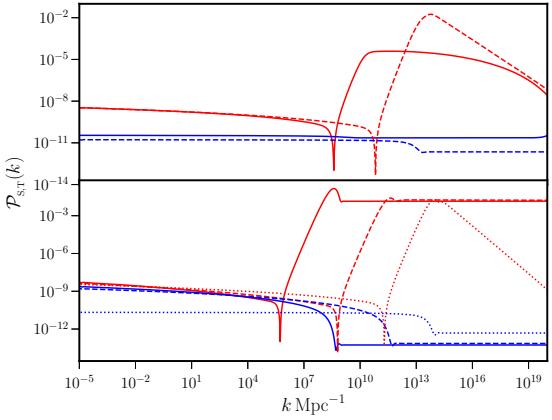

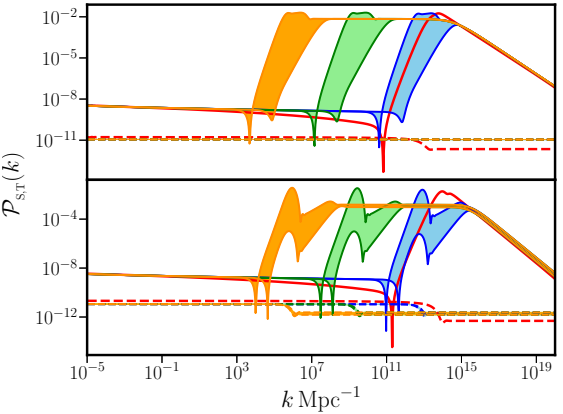

The scalar and the tensor power spectra arising in the various inflationary models (in red and blue on the left) and the reconstructed scenarios (in blue, green and orange, on the right)[18].

[18] H. V. Ragavendra, P. Saha, L. Sriramkumar and J. Silk, Phys. Rev. D **103**, 083510 (2021).

The two-field model of interest

It has been noticed that two scalar fields ϕ and χ governed by the following action:

$$S[\phi,\chi] = \int \mathrm{d}^4x\,\sqrt{-g}\,\left[-\frac{1}{2}\,\partial^\mu\phi\,\partial_\mu\phi - \frac{f(\phi)}{2}\,\partial^\mu\chi\,\partial_\mu\chi - V(\phi,\chi)\right]$$

described by a separable potential such as

$$V(\phi,\,\chi) = V_0\,\frac{\phi^2}{\phi_0^2+\phi^2} + \frac{m_\chi^2}{2}\,\chi^2$$

and the non-canonical coupling functions

$$f_1(\phi) = \mathrm{e}^{2\,b_1\,\phi} \quad \text{or} \quad f_2(\phi) = \mathrm{e}^{2\,b_2\,\phi^2}$$

can lead to features in the scalar power spectrum[19].

[19] M. Braglia, D. K. Hazra, L. Sriramkumar and F. Finelli, JCAP **08** 025 (2020).

Behavior of the scalar fields and the first slow roll parameter

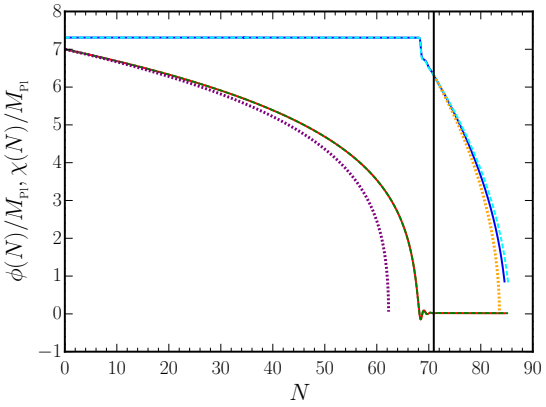

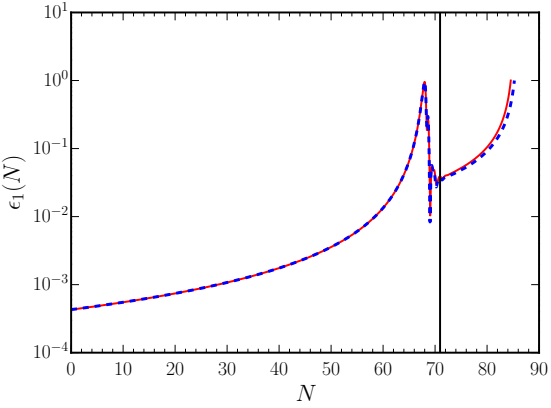

Behavior of the two scalar fields ϕ and χ (in blue and red, on the left) and the first slow roll parameter ϵ_1 (on the right) in the two field model of our interest[20]. Note that there arises a turn in the field space around $N = 70$, when the first slow roll parameter begins to decrease before increasing again, leading to the termination of inflation.

[20] M. Braglia, D. K. Hazra, F. Finelli, G. F. Smoot, L. Sriramkumar and A. A. Starobinsky, JCAP **08**, 001 (2020).

Enhanced power on small scales in two field models

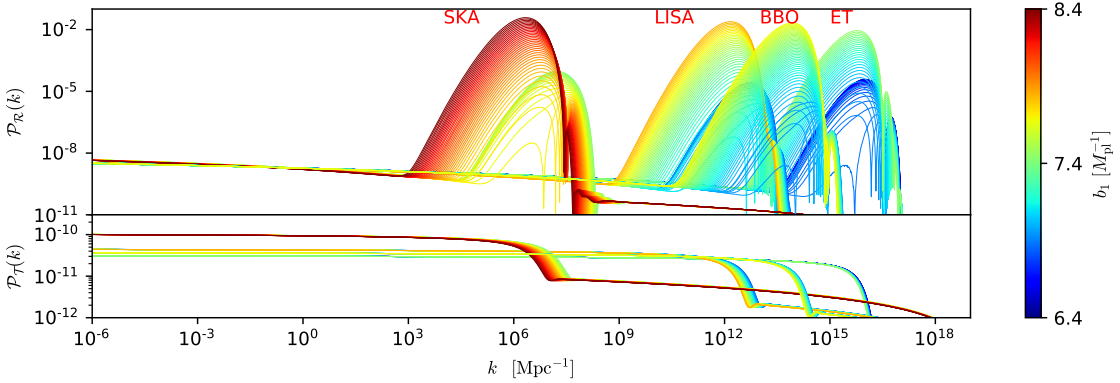

The scalar (on top) and the tensor (at the bottom) power spectra evaluated at the end of inflation have been plotted for a few different sets of initial conditions for the fields and a range of values of the parameter b_1[21].

[21] M. Braglia, D. K. Hazra, F. Finelli, G. F. Smoot, L. Sriramkumar and A. A. Starobinsky, JCAP **08**, 001 (2020).

$f_{\rm PBH}(M)$ in ultra slow roll and punctuated inflation

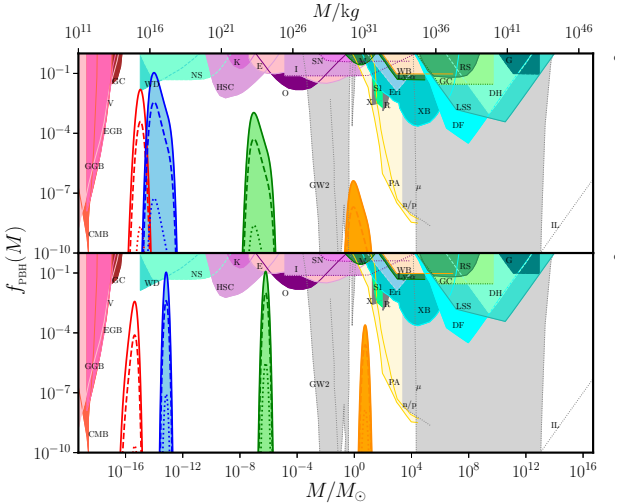

The fraction of PBHs contributing to the cold dark matter density today $f_{\rm PBH}(M)$ has been plotted for different models, viz. USR2 (on top, in red) and PI3 (at the bottom, in red)[22].

[22] H. V. Ragavendra, P. Saha, L. Sriramkumar and J. Silk, Phys. Rev. D **103**, 083510 (2021).

Illustrating the $f_{\rm PBH}(M) \propto M^{-1/2}$ behavior

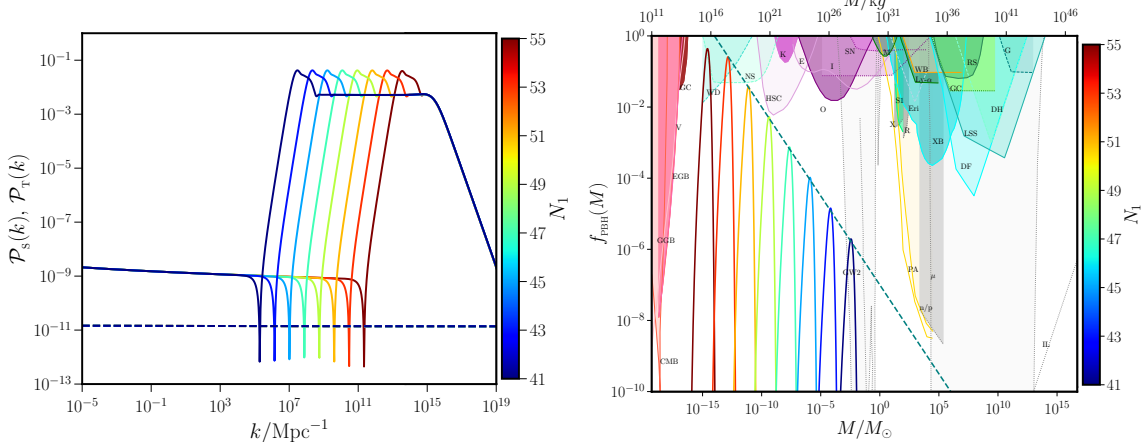

The quantity $f_{\rm PBH}(M)$ (on the right) corresponding to scalar spectra generated in the reconstructed scenarios (on the left) is illustrated. We find that $f_{\rm PBH}(M)$ behaves as $M^{-1/2}$ (in dashed teal, on the right), as expected[23].

[23] H. V. Ragavendra and L. Sriramkumar, Galaxies **11**, 34 (2023).

$f_{\rm PBH}(M)$ in the two-field model

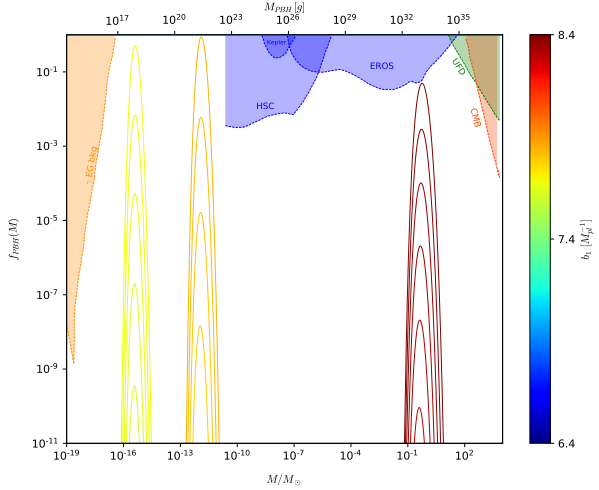

The fraction of PBHs contributing to the dark matter density today $f_{\rm PBH}(M)$ in the two-field model of our interest[24].

[24] M. Braglia, D. K. Hazra, F. Finelli, G. F. Smoot, L. Sriramkumar and A. A. Starobinsky, JCAP **08**, 001 (2020).

$\Omega_{\rm GW}(f)$ in ultra slow roll and punctuated inflation

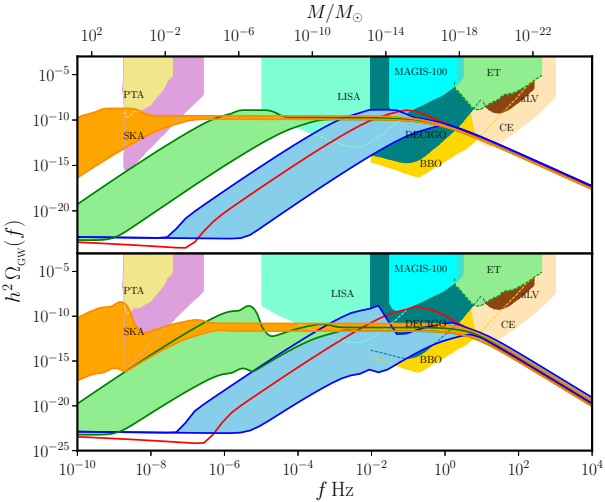

The dimensionless spectral density of GWs $\Omega_{\rm GW}(f)$ arising in the models of USR2 (in red, on top) as well as PI3 (in red, at the bottom)[25].

[25] H. V. Ragavendra, P. Saha, L. Sriramkumar and J. Silk, Phys. Rev. D **103**, 083510 (2021).

$\Omega_{\rm GW}(f)$ in the two-field model

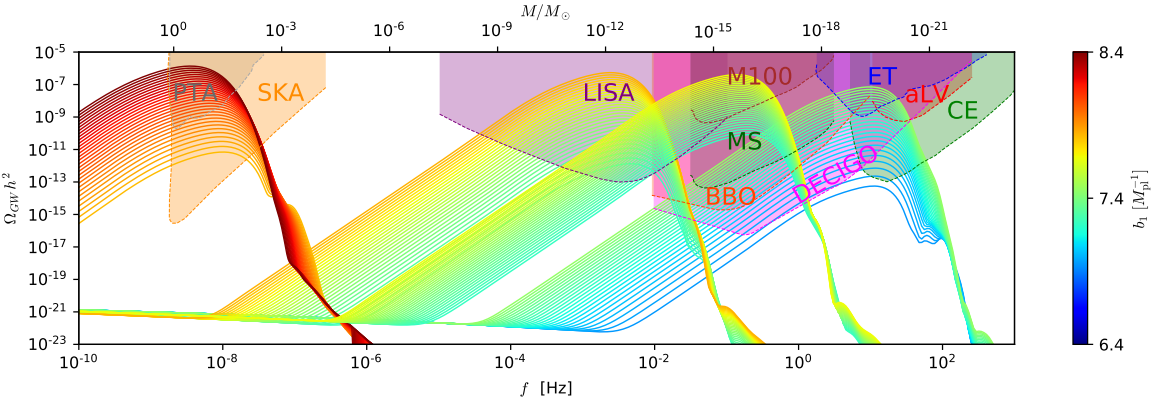

The dimensionless spectral density of GWs $\Omega_{\rm GW}(f)$ arising in the two-field model has been plotted for a set of initial conditions for the background fields as well as a range of values of the parameter b_1[26].

[26] M. Braglia, n D. K. Hazra, F. Finelli, G. F. Smoot, L. Sriramkumar and A. A. Starobinsky, JCAP **08**, 001 (2020).

Plan of the talk

Hellings-Downs curve

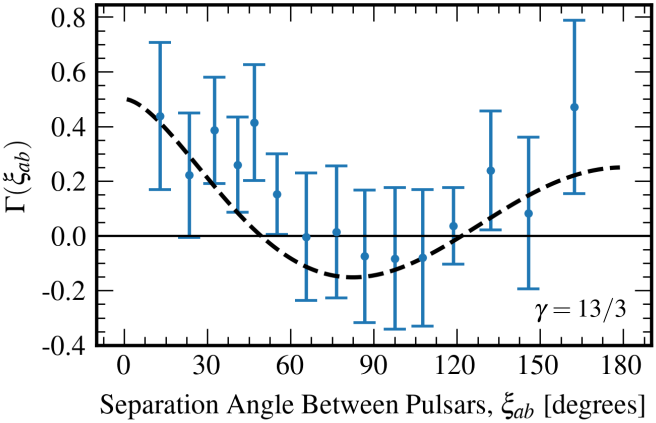

The inter-pulsar correlations measured from 2,211 distinct pairings in the 67-pulsar array of the NANOGrav 15-year data. The dashed black line shows the Hellings-Downs correlation pattern[27].

[27] NANOGrav Collaboration (G. Agazie *et al.*), Astrophys. J. Lett. **951**, 1 (2023); For related discussion, see J. Yokoyama, arXiv:2105.07629 [gr-qc].

Constraints on the spectral amplitude and index of GWs

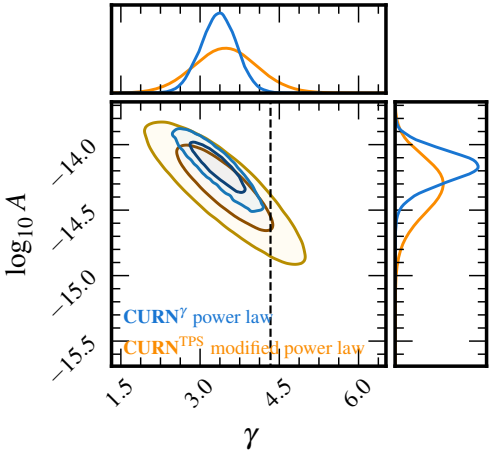

Constraints on the amplitude A and the index γ of the stochastic background of GWs from the NANOGrav 15-year data[28].

[28] NANOGrav Collaboration (G. Agazie *et al.*), Astrophys. J. Lett. **951**, 1 (2023).

Stochastic GW background observed by pulsar timing arrays (PTAs)

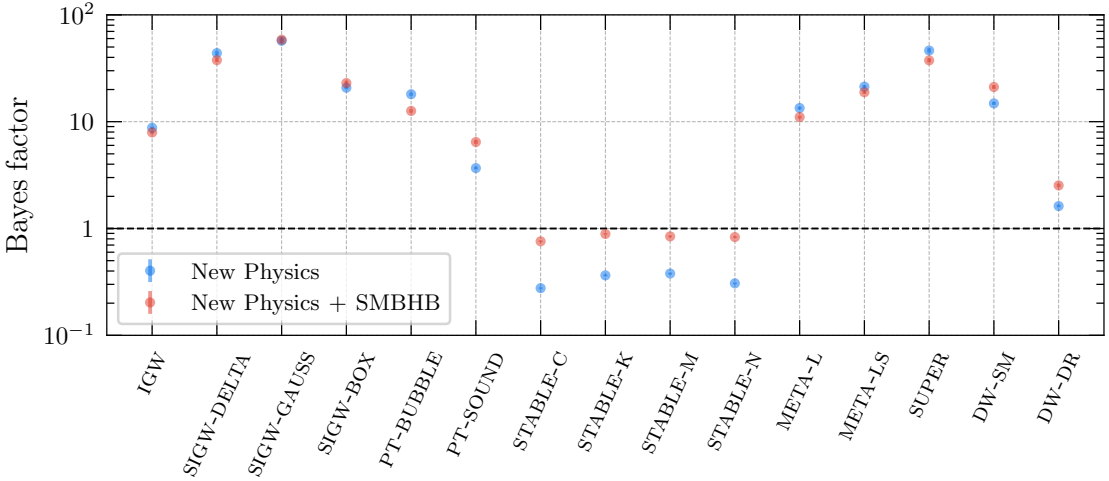

The Bayesian evidence for a variety of astrophysical and cosmological sources for the stochastic GW background suggested by the observations of the PTAs[29].

[29] NANOGrav Collaboration (G. Agazie *et al.*), Astrophys. J. Lett. **951**, 1 (2023).

Shape of the inflationary scalar power spectrum

We assume that the inflationary scalar power spectrum is given by[30]

$$\mathcal{P}_{\mathcal{R}}(k) = A_{\rm s}\left(\frac{k}{k_*}\right)^{n_{\rm S}-1} + A_0 \begin{cases} \left(\dfrac{k}{k_{\rm peak}}\right)^4 & k \leq k_{\rm peak} \\ \left(\dfrac{k}{k_{\rm peak}}\right)^{n_0} & k \geq k_{\rm peak} \end{cases},$$

where $A_{\rm s}$ and $n_{\rm S}$ are the amplitude and spectral index of the power spectrum at the CMB pivot scale of $k_* = 0.05\,{\rm Mpc}^{-1}$.

We set the reheating temperature to the rather low value of $T_{\rm re} = 50\,{\rm MeV}$.

We shall assume that the threshold value of the density contrast for the formation of PBHs is given by[31]:

$$\delta_{\rm c}^{\rm an} = \frac{3\,(1+w_{\rm re})}{5+3\,w_{\rm re}}\,\sin^2\left(\frac{\pi\,\sqrt{w_{\rm re}}}{1+3\,w_{\rm re}}\right).$$

[30] For other forms of spectra, see G. Domènech, S. Pi, A. Wang and J. Wang, arXiv:2402.18965 [astro-ph.CO].

[31] In this context, see T. Harada, C.-M. Yoo, and K. Kohri, Phys. Rev. D **88**, 084051 (2013).

Formation of PBHs during the phase of reheating

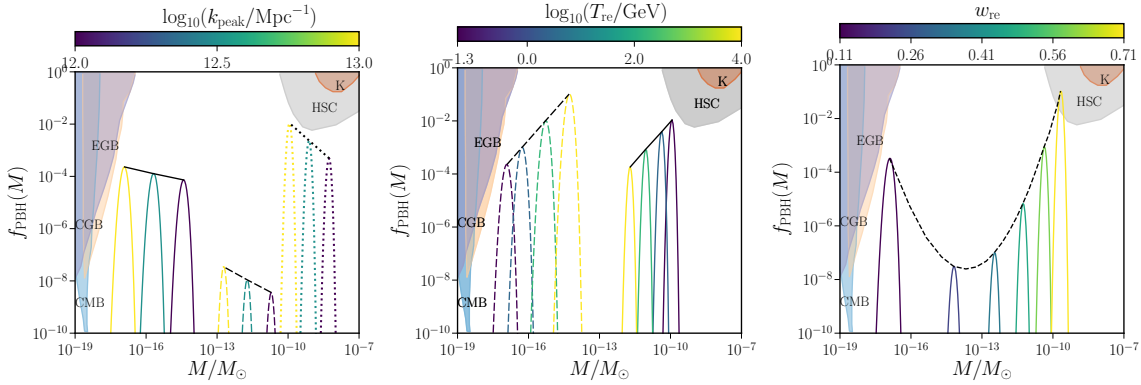

The quantity $f_{\rm PBH}$ is plotted as a function $M/M_\odot$ for a range of $k_{\rm peak}$, $T_{\rm re}$ and $w_{\rm re}$ (in the left, middle and right panels).

Generation of secondary GWs during the epoch of reheating

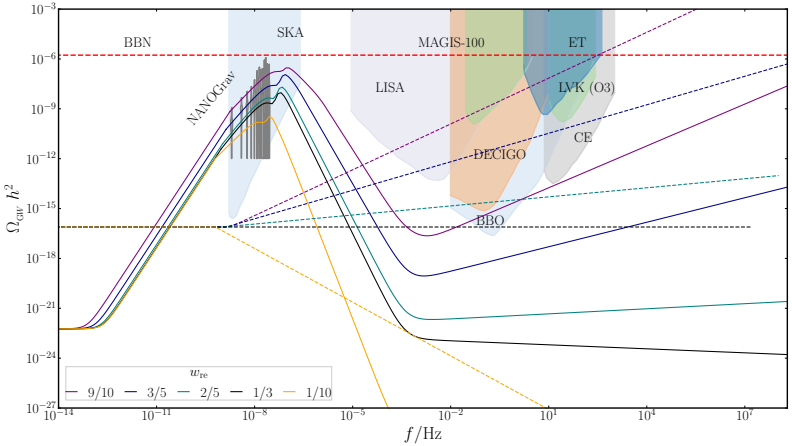

Epoch of reheating

The dimensionless spectral energy density of primary and secondary GWs today $\Omega_{\rm GW}(f)$ is plotted for a given reheating temperature and different values of the parameter describing the equation of state during reheating[32].

[32] S. Maity, N. Bhaumik, Md. R. Haque, D. Maity and L. Sriramkumar, arXiv:2403.16963 [astro-ph.CO].

Best-fit values

Model	Parameter	Prior	Mean value		
R4pF	$\log_{10}\left(\frac{k_{\rm peak}}{\rm Mpc^{-1}}\right)$	$[6, 9]$	$7.62^{+0.35}_{-0.41}$		
	$\log_{10}(A_0)$	$[-3, 0]$	$-1.23^{+0.38}_{-0.66}$		
	$w_{\rm re}$	$[0.1, 0.9]$	0.52 ± 0.23		
	n_0	$[-3.0, -1.5]$	-2.26 ± 0.43		
R3pF	$\log_{10}\left(\frac{k_{\rm peak}}{\rm Mpc^{-1}}\right)$	$[6, 9]$	$7.54^{+0.36}_{-0.44}$		
	$\log_{10}(A_0)$	$[-3, 0]$	$-1.26^{+0.26}_{-0.64}$		
	$w_{\rm re}$	$[0.1, 0.9]$	$0.55^{+0.39}_{-0.14}$		
			$\mathbf{0.5\,\delta_c^{an}}$	$\boldsymbol{\delta_c^{an}}$	$\mathbf{1.5\,\delta_c^{an}}$
R3pB	$\log_{10}\left(\frac{M}{M_\odot}\right)$	$[-6, 3.5]$	$-0.12^{+0.28}_{-0.15}$	$-1.18^{+0.35}_{-0.39}$	$-1.85^{+0.49}_{-0.30}$
	$\log_{10}(f_{\rm PBH})$	$[-20, 0]$	$-0.67^{+0.68}_{-0.16}$	$-6.6^{+6.5}_{-1.9}$	$-10.2^{+8.2}_{-9.6}$
	$w_{\rm re}$	$[0.1, 0.9]$	$0.78^{+0.11}_{-0.030}$	$0.66^{+0.23}_{-0.19}$	0.55 ± 0.17
R2pB	$\log_{10}\left(\frac{M}{M_\odot}\right)$	$[-6, 3.5]$	$-0.24^{+0.38}_{-0.45}$	$-1.60^{+0.16}_{-0.14}$	$-2.45^{+0.20}_{-0.13}$
	$w_{\rm re}$	$[0.1, 0.9]$	$0.77^{+0.13}_{-0.038}$	0.59 ± 0.16	$0.464^{+0.095}_{-0.25}$

The best-fit values arrived at upon comparison with the NANOGrav 15-year data.

Constraints on the epoch of reheating

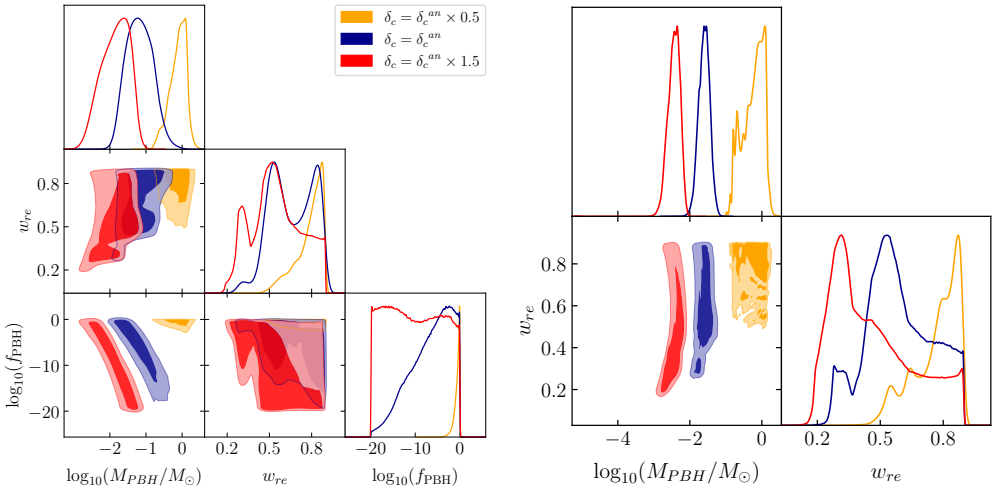

Constraints on the parameters in the models `R3pB` (on the left) and `R2pB` (on the right), arrived at upon comparison with the NANOGrav 15-year data[33].

[33] S. Maity, N. Bhaumik, Md. R. Haque, D. Maity and L. Sriramkumar, arXiv:2403.16963 [astro-ph.CO].

Generation of secondary GWs during the epoch of reheating

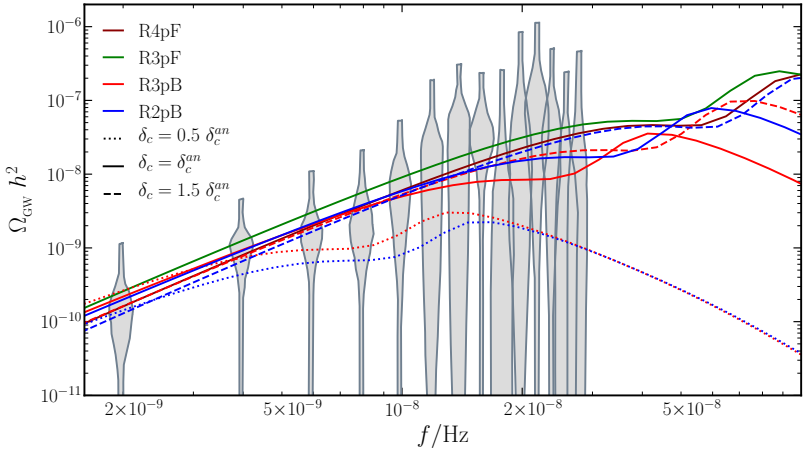

▸ Epoch of reheating

The dimensionless spectral energy density of the secondary GWs today $\Omega_{\rm GW}(f)$ is plotted for a given reheating temperature and the best-fit values of the parameters in the different models[34].

[34] S. Maity, N. Bhaumik, Md. R. Haque, D. Maity and L. Sriramkumar, arXiv:2403.16963 [astro-ph.CO].

Extent of PBHs formed

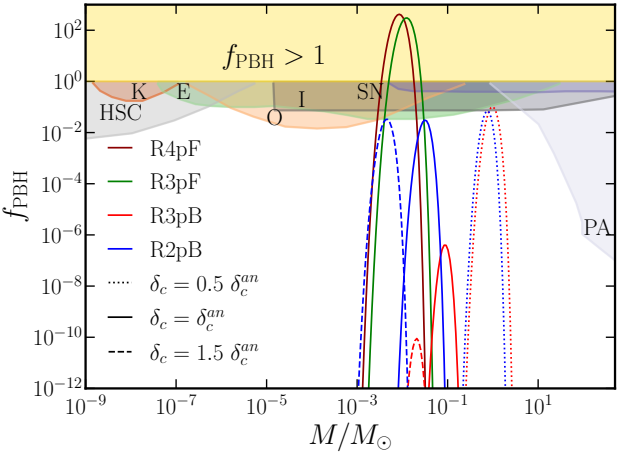

The fraction of PBHs that constitute the dark matter density today, viz. $f_{\rm PBH}(M)$ is plotted for a given reheating temperature and the best-fit values of the parameters in the different models[35].

[35] S. Maity, N. Bhaumik, Md. R. Haque, D. Maity and L. Sriramkumar, arXiv:2403.16963 [astro-ph.CO].

Bayesian evidence

Model X	Model Y	$\mathrm{BF}_{Y,X}$		
		$\delta_{\rm c} = 0.5\,\delta_{\rm c}^{\rm an}$	$\delta_{\rm c} = \delta_{\rm c}^{\rm an}$	$\delta_{\rm c} = 1.5\,\delta_{\rm c}^{\rm an}$
SMBHB	R2pB	$1.7 \pm .06$	260.04 ± 19.21	350.61 ± 27.36

The Bayesian factors $\mathrm{BF}_{Y,X}$ for the model R2pB that invokes primordial physics as the source of the stochastic GW background observed by the NANOGrav 15-year data, when compared to the astrophysical SMBHB model.

Bayesian factors $\mathrm{BF}_{Y,X}$ that far exceed unity indicate strong evidence for the model Y with respect to the model X.

Clearly, when $\delta_{\rm c} = \delta_{\rm c}^{\rm an}$ and $\delta_{\rm c} = 1.5\,\delta_{\rm c}^{\rm an}$, the NANOGrav 15-year data strongly favors the model R2pB when compared to the SMBHM model.

Plan of the talk

Template bispectra

For comparison with the observations, the scalar bispectrum is often expressed in terms of the parameters $f_{\rm NL}^{\rm loc}$, $f_{\rm NL}^{\rm eq}$ and $f_{\rm NL}^{\rm orth}$ as follows:

$$\mathcal{B}(\boldsymbol{k}_1, \boldsymbol{k}_2, \boldsymbol{k}_3) = f_{\rm NL}^{\rm loc}\, \mathcal{B}_{\rm loc}(\boldsymbol{k}_1, \boldsymbol{k}_2, \boldsymbol{k}_3) + f_{\rm NL}^{\rm eq}\, \mathcal{B}_{\rm eq}(\boldsymbol{k}_1, \boldsymbol{k}_2, \boldsymbol{k}_3) + f_{\rm NL}^{\rm orth}\, \mathcal{B}_{\rm orth}(\boldsymbol{k}_1, \boldsymbol{k}_2, \boldsymbol{k}_3).$$

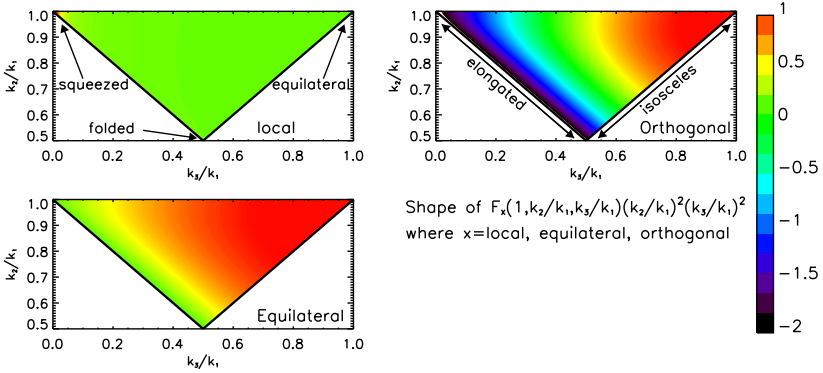

Illustration of the three template basis bispectra[36].

[36] E. Komatsu, Class. Quantum Grav. **27**, 124010 (2010).

Constraints on the scalar non-Gaussianity parameters

The constraints on the primordial values of the non-Gaussianity parameters from the Planck data are as follows[37]:

$$
\begin{aligned}
f_{\rm NL}^{\rm loc} &= -0.9 \pm 5.1, \\
f_{\rm NL}^{\rm eq} &= -26 \pm 47, \\
f_{\rm NL}^{\rm ortho} &= -38 \pm 24.
\end{aligned}
$$

These constraints imply that slowly rolling single field models involving the canonical scalar field which are favored by the data at the level of power spectra are also consistent with the data at the level of non-Gaussianities.

[37] Planck Collaboration (Y. Akrami *et al.*), Astron. Astrophys. **641**, A9 (2020).

The shape of the slow roll bispectrum

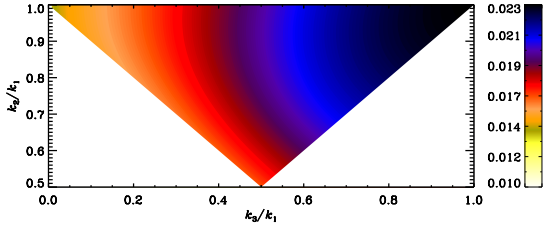

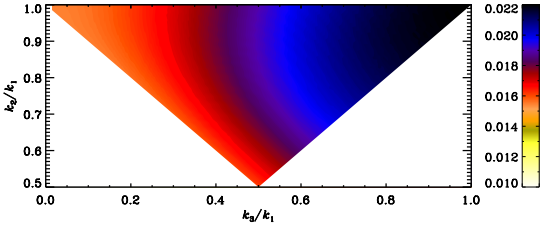

The non-Gaussianity parameter $f_{\rm NL}$, evaluated in the slow roll approximation (analytically on the left and numerically on the right), has been plotted as a function of k_3/k_1 and k_2/k_1 for the case of the popular quadratic potential[38]. Note that the non-Gaussianity parameter peaks in the equilateral limit wherein $k_1 = k_2 = k_3$. In slow roll scenarios involving the canonical scalar field, the largest value of $f_{\rm NL}$ is found to be of the order of the first slow roll parameter ϵ_1.

[38] D. K. Hazra, L. Sriramkumar and J. Martin, JCAP **05**, 026, (2013).

The scalar bispectrum in ultra slow roll and punctuated inflation

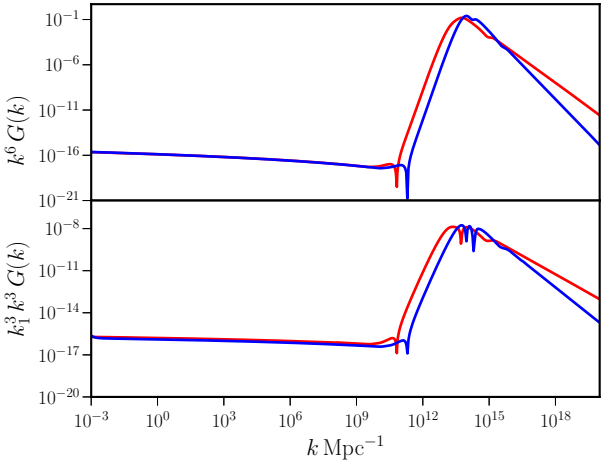

The amplitude of the dimensionless scalar bispectra is plotted in the equilateral (on top) and squeezed limits (at the bottom) for the models USR2 (in red) and PI3 (in blue). The bispectra have approximately the same shape as the corresponding power spectra[39].

[39] H. V. Ragavendra, P. Saha, L. Sriramkumar and J. Silk, Phys. Rev. D **103**, 083510 (2021).

$f_{\rm NL}$ in ultra slow roll and punctuated inflation

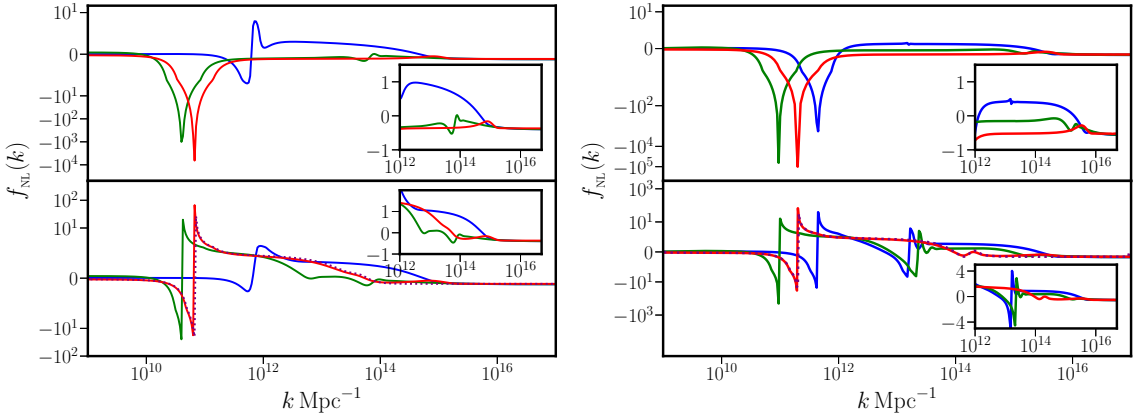

The scalar non-Gaussianity parameter $f_{\rm NL}$ is plotted in the equilateral (on top) and the squeezed (at the bottom) limits for the models of USR2 and PI3 (in red, on the left and the right) and the reconstructed scenarios RS1 and RS2 (in blue and green, on the left and the right).

Complete shape of $f_{\rm NL}$ in ultra slow roll inflation

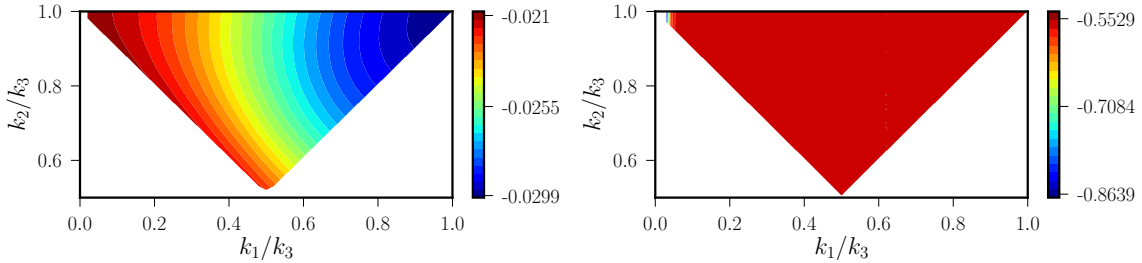

The shape of the scalar non-Gaussianity parameter $f_{\rm NL}$ in a ultra slow roll scenario around the pivot scale (on the left) and around the peak in the scalar power spectrum (on the right)[40].

[40] H. V. Ragavendra and L. Sriramkumar, Galaxies **11**, 34 (2023).

Plan of the talk

The action describing the scalar perturbations at the quartic order

There have been recent efforts to understand if the loop corrections to the inflationary scalar power spectrum remain small if there is an enhancement in power on small scales[41].

In the action describing the scalar perturbations, at the quartic order, the dominant term is given by[42]

$$S^{(4)}[\zeta(\eta,\boldsymbol{x})] = \frac{1}{72}\int \mathrm{d}\eta \int \mathrm{d}^3\boldsymbol{x}\, a^4\, \epsilon_1\, \epsilon_2\, \epsilon_3\, \epsilon_4\, \epsilon_5\, V\, \zeta^4.$$

The corresponding interaction Hamiltonian can be determined to be

$$H^{(4)}_{\rm int} = -\frac{1}{72}\int \mathrm{d}^3\boldsymbol{x}\, a^4\, \epsilon_1\, \epsilon_2\, \epsilon_3\, \epsilon_4\, \epsilon_5\, V\, \zeta^4.$$

[41] See, for example, J. Kristiano and J. Yokoyama, Phys. Rev. Lett. **132**, 221003 (2024); A. Riotto, arXiv:2301.00599; H. Firouzjahi and A. Riotto, JCAP **02**, 021 (2024); G. Franciolini, A. J. Iovino, M. Taoso, and A. Urbano, arXiv:2305.03491.

[42] E. Dimastrogiovanni and N. Bartolo, JCAP **11**, 016 (2008).

Smoothing the transitions

In a SR-USR-SR scenario, we smooth the transitions by replacing the delta functions we encounter by a Gaussian as follows:

$$\delta^{(1)}(\eta-\tilde{\eta}) = \frac{1}{\sqrt{\pi}\,\Delta\eta}\,\mathrm{e}^{-\frac{(\eta-\tilde{\eta})^2}{\Delta\eta^2}},$$

where $\tilde{\eta}$ is the point of transition and $\Delta\eta$ denote the sharpness of transition[43].

In such a case, we can express the time-derivative of the second SR parameter ϵ_2 as

$$\epsilon_2' = \begin{cases} \dfrac{\epsilon_2^{\mathrm{II}}}{\sqrt{\pi}\,\Delta\eta}\,\mathrm{e}^{-\frac{(\eta-\eta_1)^2}{\Delta\eta^2}} & \text{around } \eta_1, \\ -\dfrac{\epsilon_2^{\mathrm{II}}}{\sqrt{\pi}\,\Delta\eta}\,\mathrm{e}^{-\frac{(\eta-\eta_2)^2}{\Delta\eta^2}} & \text{around } \eta_2. \end{cases}$$

The higher order SR parameters ϵ_3, ϵ_4 and ϵ_5 can then be obtained to be

$$\epsilon_3 = \mp\frac{\eta}{\sqrt{\pi}\,\Delta\eta}\,\mathrm{e}^{-\frac{(\eta-\eta_{1,2})^2}{\Delta\eta^2}},\quad \epsilon_4 = -1+\frac{2\,\eta\,(\eta-\eta_{1,2})}{\Delta\eta^2},\quad \epsilon_5 = \frac{2\,\eta\,(2\,\eta-\eta_{1,2})}{\Delta\eta^2-2\,\eta\,(\eta-\eta_{1,2})}.$$

[43] S. Maity, H. V. Ragavendra, S. K. Sethi and L. Sriramkumar, JCAP **05**, 046 (2024).

Corrections to power spectrum due to the dominant term

In the in-in formalism, at the leading order, the two point correlation function due to the interaction Hamiltonian $H_{\rm int}^{(4)}$ is given by the expression

$$\langle\hat{\zeta}_{\boldsymbol{k}}(\eta_{\rm e})\,\hat{\zeta}_{\boldsymbol{k}'}(\eta_{\rm e})\rangle = \langle\hat{\zeta}_{\boldsymbol{k}}(\eta_{\rm e})\,\hat{\zeta}_{\boldsymbol{k}'}(\eta_{\rm e})\rangle - i\,\langle[\hat{\zeta}_{\boldsymbol{k}}(\eta_{\rm e})\,\hat{\zeta}_{\boldsymbol{k}'}(\eta_{\rm e}), \int {\rm d}\eta\,\mathcal{T}\{\hat{H}_{\rm int}^{(4)}(\eta)\}]\rangle.$$

In the vacuum, the dominant loop contribution can be written as as

$$\langle\hat{\zeta}_{\boldsymbol{k}}(\eta_{\rm e})\,\hat{\zeta}_{\boldsymbol{k}'}(\eta_{\rm e})\rangle_{\rm C} \simeq \delta^{(3)}(\boldsymbol{k}+\boldsymbol{k}')\left\{\frac{i}{6}\,f_k(\eta_{\rm e})\,f_{k'}(\eta_{\rm e})\int {\rm d}\eta\,a^4\,\epsilon_1\,\epsilon_2\,\epsilon_3\,\epsilon_4\,\epsilon_5\,V\,f_k^*(\eta)\,f_{k'}^*(\eta)\right.$$
$$\left.\times\int\frac{{\rm d}^3\boldsymbol{q}}{(2\,\pi)^3}|f_q(\eta)|^2 + \text{ complex conjugate}\right\}$$

so that the correction to the scalar power spectrum is given by

$$\mathcal{P}_{\rm C}^{(4)}(k) = \frac{i}{6}\left(\frac{k^3}{2\,\pi^2}\right)f_k^2(\eta_{\rm e})\int {\rm d}\eta\,a^4\,\epsilon_1\,\epsilon_2\,\epsilon_3\,\epsilon_4\,\epsilon_5\,V\,[f_k^*(\eta)]^2\int {\rm d}\ln q\,\mathcal{P}_{\rm S}(q,\eta)$$
$$+ \text{ complex conjugate.}$$

Typical loop contributions to the power spectrum

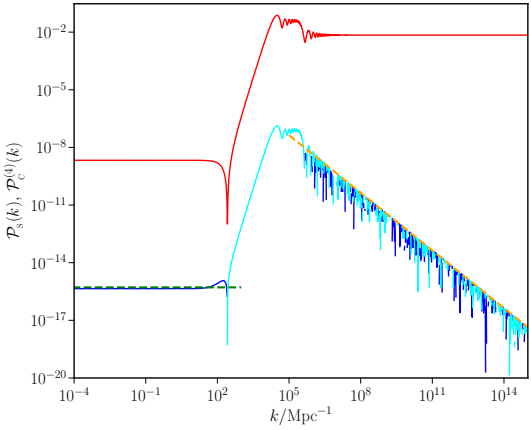

The power spectrum at the first order $\mathcal{P}_{\rm S}(k)$ (in red) and the loop contributions $\mathcal{P}_{\rm C}^{(4)}(k)$ (in blue) have been illustrated for the following parameters: $H = 1.3 \times 10^{-5}\, M_{\rm Pl}$, $\epsilon_{1{\rm i}} = 10^{-3}$,$\epsilon_2^{\rm II} = -6$, $\Delta\eta = 10^{-3}\,{\rm Mpc}$, $k_1 = 10^4\,{\rm Mpc}^{-1}$, $\Delta N = 2.5$, $k_{\rm min} = 10^{-6}\,{\rm Mpc}^{-1}$, and $k_{\rm max} = 10^{20}\,{\rm Mpc}^{-1}$. We have also indicated the domains where $\mathcal{P}_{\rm C}^{(4)}(k)$ negative (in cyan).

Loop contributions for late onset of USR

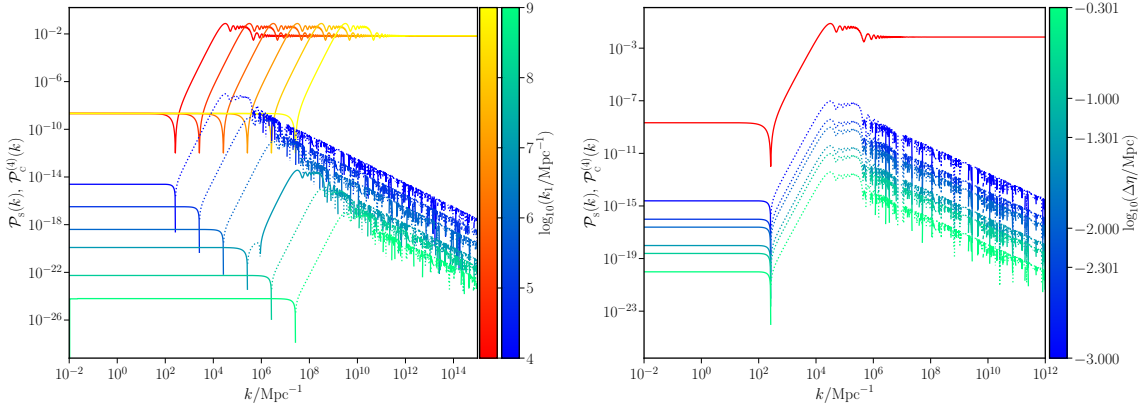

The power spectrum at the first order $\mathcal{P}_{\rm S}(k)$ and the loop contributions $\mathcal{P}_{\rm C}^{(4)}(k)$ have been illustrated for different values of k_1 (on the left) and different values of $\Delta\eta$ (on the right).

Loop contributions for intermediate and early onsets of USR

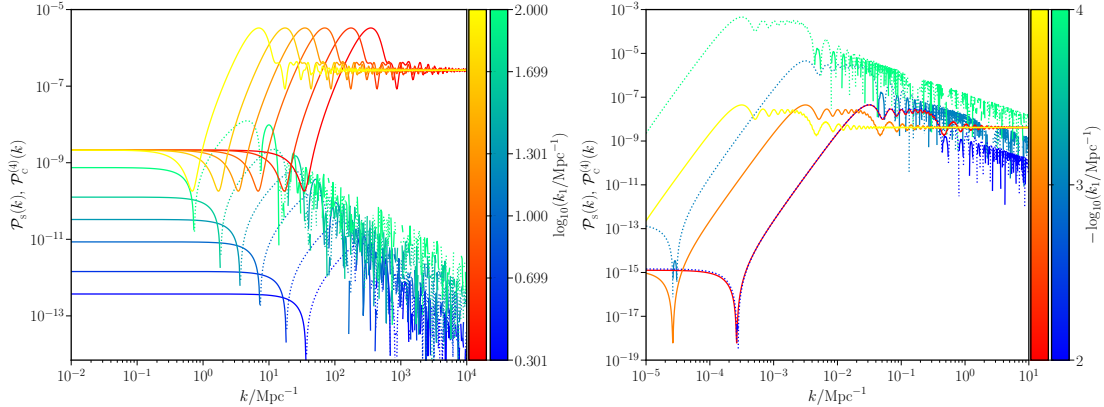

The power spectrum at the first order $\mathcal{P}_{\rm S}(k)$ and the loop contributions $\mathcal{P}_{\rm C}^{(4)}(k)$ have been illustrated for intermediate (on the left) and early (on the right) onsets of USR. Note that, as the USR sets in earlier and earlier, the contributions from the loops prove to be larger and larger.

Contributions for early USR: Effects of duration and sharpness

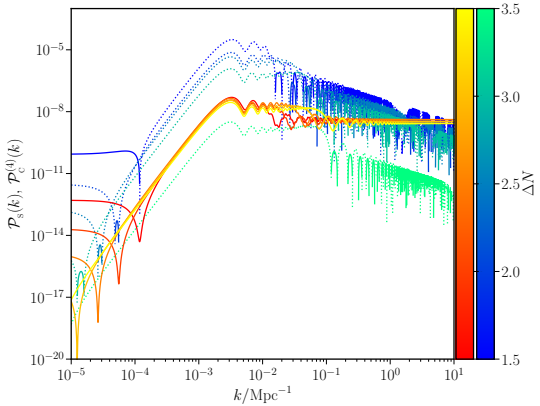

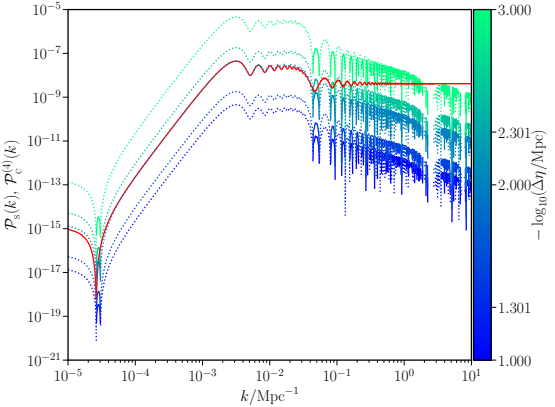

We find that the earlier is the phase of USR and the sharper is the transition, the larger are the loop contributions to the scalar power spectrum[44]. These raise the specter of the breakdown of perturbation theory!

[44] S. Maity, H. V. Ragavendra, S. K. Sethi and L. Sriramkumar, JCAP **05**, 046 (2024).

Plan of the talk

Outlook

- If one of the future CMB missions—such as LiteBIRD (Lite, Light satellite for the studies of B-mode polarization and Inflation from cosmic background Radiation Detection), Primordial Inflation Explorer (PIXIE) or Exploring Cosmic History and Origin (ECHO, a proposed Indian effort)—detect the signatures of the primordial GWs, it will help us arrive at strong constraints on the dynamics during inflation and reheating.
- The observations by LIGO have opened up a new window to observe the universe.
- The observations by the PTAs and their possible implications for the stochastic GW background offer a wonderful opportunity to understand the physics operating over a wider range of scales in the early universe. During the coming decades, GW observatories such as the Laser Interferometer Space Antenna (LISA), Einstein Telescope and Cosmic Explorer, can be expected to provide us with an unhindered view of the primordial universe.
- On the theoretical front, the role of non-Gaussianities in the formation of PBHs and the generation of GWs and the corrections to the power spectra due to the higher order terms in the action, remain to be understood satisfactorily.

Collaborators I

Matteo Braglia

Dhiraj Hazra

Fabio Finelli

George Smoot

Alexei Starobinsky

H. V. Ragavendra

Pankaj Saha

Joseph Silk

Collaborators II

Md. Riajul Haque

Debaprasad Maity

Tanmoy Paul

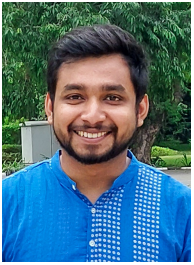

Suvashis Maity

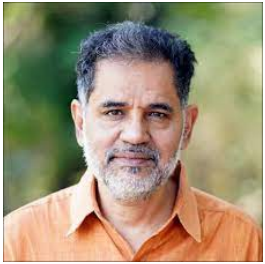

Shiv Kumar Sethi

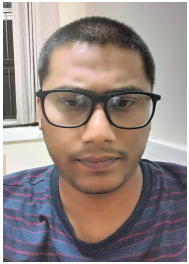

Nilanjandev Bhaumik

Thank you for your attention